*Optica Applicata, Vol. XLIX, No. 4, 2019*
DOI: 10.37190/oa190409

# Numerical modeling of field-assisted $Ag^+$–$Na^+$ ion-exchanged channel waveguides using varied explicit space charge density approach

Piotr MROZEK

Faculty of Mechanical Engineering, Bialystok University of Technology,
Wiejska 45C, 15-351 Bialystok, Poland; p.mrozek@pb.edu.pl

This article presents a numerical model of field-assisted $Ag^+$–$Na^+$ ion exchange in glass, used to determine $Ag^+$ ion concentration contours in cross-sections of channel waveguides. Space charge density was used as a modeling parameter, with different values adopted separately under the mask and in the region of the mask window. Based on the results of simulations, it can be stated that the space charge distribution under the mask has a decisive influence on the diffusion range of $Ag^+$ ions into the glass and on the shape of silver ion concentration contours corresponding to the maximum range of $Ag^+$ ions diffusion. Charge generated within the diffusive structure influences the shape of silver ion concentration contours near the mask's edge and affects the thickness of the polarized layer under the mask within the waveguide's optical structure. Modeling results indicate a significant influence of factors affecting space charge density distribution in glass on the results of forming channel waveguides in the field-assisted process.

Keywords: numerical modeling, channel waveguide, field-assisted ion exchange.

## 1. Introduction

$Ag^+$–$Na^+$ ion exchange is a cheap and productive method of fabricating active and passive planar integrated optical devices [1–3]. Waveguides produced in the superficial layer of a glass substrate are a basic structure in many different types of optical devices such as couplers, dividers, amplifiers, *etc*. [4–7]. One useful method of fabricating waveguide structures is field-assisted ion exchange from melted salt or a solid metallic source [1–3], with the use of a window in a metallic or dielectric mask deposited on the surface of glass (Fig. 1). Numerical modeling is a useful tool for designing and testing the structural and functional features of waveguides produced by means of this method [2, 8–11]. In recent years, a numerical model has been presented and confronted with experimental data [12–14], explicitly accounting for the presence of space charge induced in two areas: in the surface layer of glass under the entire mask and in the optical structure formation region neighboring the mask window. Space charge distribution plays a central role in shaping electric field distribution, and the range of $Ag^+$ ion migration results, above all, from flowing of ions in the field within the glass. Boundary

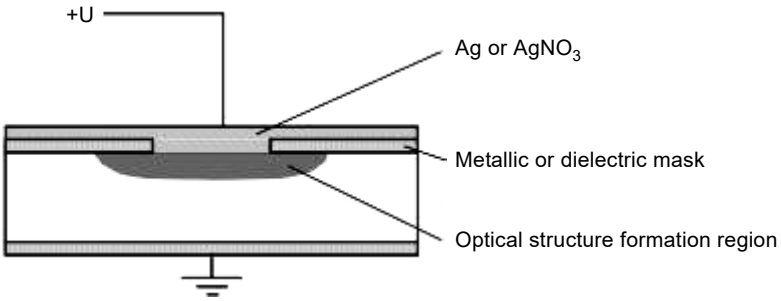


Fig. 1. Field-assisted $Ag^+$–$Na^+$ ion exchange process.

conditions of electrical potential distribution were adopted in the model in accordance with physically implemented conditions. The addition of other ions besides $Ag^+$ and $Na^+$ was also assumed to affect space charge density distribution in the glass over the course of optical structure formation. In particular, the involvement of $H^+$ ions, among others, in the redistribution of space charge and the electric field distribution arising therefrom was accounted for and modeled using the solution of Poisson's equation [12–14]. The assumptions described above were not taken into consideration in many previously published works [2, 8–11]. In these works, the solution of Laplace's equation for boundary conditions accounting for anode potential only in the mask's window was used to shape electric field distribution in glass.

In works describing the results of the proposed model [12, 13], attention was paid to the fact that the nature of phenomena affecting space charge density varies between the two aforementioned, characteristic areas where space charge is present. Modeling results indicate that a negative charge of relatively high density and a stationary spatial distribution accumulates under the mask, however for the most part, it is situated far from the formed waveguide structure. Negative space charge is also generated directly in the area of the optical structure, however it is of significantly lesser density than under the mask and is characterized by distribution that changes dynamically as $Ag^+$ ions migrate. It was determined that a simultaneous change of charge density in both of these areas has a strong influence on electric field distribution and the range of $Ag^+$ ion diffusion as well as on the shape of the concentration contours of $Ag^+$ ions in the waveguide, which earlier models did not describe. However, the adopted method of quantitatively determining the space charge density, identical in both of the aforementioned areas, did not allow for investigation of the effect of charge distribution in each of these regions separately on the migration range of $Ag^+$ ions and on the shape of silver concentration contours in the produced waveguide. Therefore, the influence of space charge distribution on the shape of the waveguide's diffusion profile was not unambiguously formulated.

This paper proposes a method of modeling that allows for investigation of the effect of space charge distribution, separately in the two areas described above, on the migration range of $Ag^+$ ions and on the shape of silver concentration contours in the channel waveguide.

## 2. Brief characterization of the numerical model

### 2.1. Equations of the mathematical model

In the proposed model [12–14], two separately formulated equations of Fick's second law for $Ag^+$ and $Na^+$ ions are used:

$$\frac{\partial C_{\mathrm{Ag(Na)}}}{\partial t} = D_{\mathrm{Ag(Na)}} \nabla^2 C_{\mathrm{Ag(Na)}} - \mu_{\mathrm{Ag(Na)}} (C_{\mathrm{Ag(Na)}} \nabla \cdot \mathbf{E} + \mathbf{E} \cdot \nabla C_{\mathrm{Ag(Na)}}) \tag{1}$$

where: $C_{\mathrm{Ag(Na)}}$ are absolute concentrations of $Ag^+$ and $Na^+$ ions, respectively, $t$ – time, $D_{\mathrm{Ag(Na)}}$ – ion self-diffusion coefficient, $\mu_{\mathrm{Ag(Na)}}$ – ion mobility, $\mathbf{E}$ – total intensity of electric field in glass. The dependence between ion mobility $\mu$ and self-diffusion coefficient $D$ is described by the Nernst–Einstein equation for $Na^+$ and $Ag^+$ ions:

$$\frac{\mu_{\mathrm{Ag(Na)}}}{D_{\mathrm{Ag(Na)}}} = \frac{e}{f_{\mathrm{H}} k T} \tag{2}$$

where: $T$, $k$, $e$ are the absolute temperature, Boltzmann constant and the elementary charge, respectively, $f_{\mathrm{H}}$ is Haven's ratio. Equations (1) are used separately for the two types of ions in order to estimate space charge density $\rho_0$, related to the non-equilibrium of the sum of concentrations $C_{\mathrm{Ag}} + C_{\mathrm{Na}}$ relative to the initial value of sodium ion concentration in glass $C_0$

$$\rho_0 = (C_{\mathrm{Ag}} + C_{\mathrm{Na}} - C_0) F \tag{3}$$

where $F$ is the Faraday constant. Space charge density $\rho$ in glass, after considering migration of ions other than just $Ag^+$ and $Na^+$ ions [12–14], reducing density $\rho_0$, was accepted to be, until now

$$\rho = m\rho_0 \tag{4}$$

where $m$ is a constant coefficient (on the order of $10^{-7}$–$10^{-6}$ in simulations until now). The solution of Poisson's equation

$$\nabla^2 U = -\frac{\rho}{\varepsilon_{\mathrm{r}} \varepsilon_0} \tag{5}$$

where $\varepsilon_{\mathrm{r}}$ and $\varepsilon_0$ are, respectively, relative permittivity of glass and permittivity of vacuum, under the set boundary conditions of electrical potential $U$, and the relationship

$$\mathbf{E} = -\nabla U \tag{6}$$

make it possible to determine field intensity $\mathbf{E}$ at every point of the area required to solve Eq. (1). Equations (1)–(6) constitute the basis of the numerical model, which uses the finite difference method in simulations.

## 2.2. Shaping the distribution of space charge and electric field in glass

Data given in [15] indicate that when a mask deposited on the surface of multicomponent silicate glass containing $Na^+$ ions is positively polarized with constant electrical voltage on the order of several dozen volts, mobile $Na^+$ ions flow out from a thin region under the anode. A negative charge appears in the thin polarized layer under the blocking electrode, and the intensity of the electric field in this layer reaches a relatively high value. In effect, other, less mobile ions, typically depending on the composition of the glass: $K^+$, $Ca^{2+}$, $Mg^{2+}$, $OH^-$, $O^-$ (non-bridging oxygen) migrate in the electric field in the polarized layer. In [16, 17], great significance in space charge redistribution was also ascribed to $H^+$ ions, originating from, among other things, residual water in the surface layer of glass. As a result, it was accepted, using Eq. (4), that negative space charge in the polarized layer has relatively high density, but lower than in the situation where $Ag^+$ and $Na^+$ ions would be the only mobile ions in the glass.

If $M = D_{Ag}/D_{Na} < 1$, then the range of space charge presence in the optical structure formation region, and thus at the location where $Ag^+$–$Na^+$ ion exchange occurs through the mask window, reaches much deeper than the area of the polarized layer under the

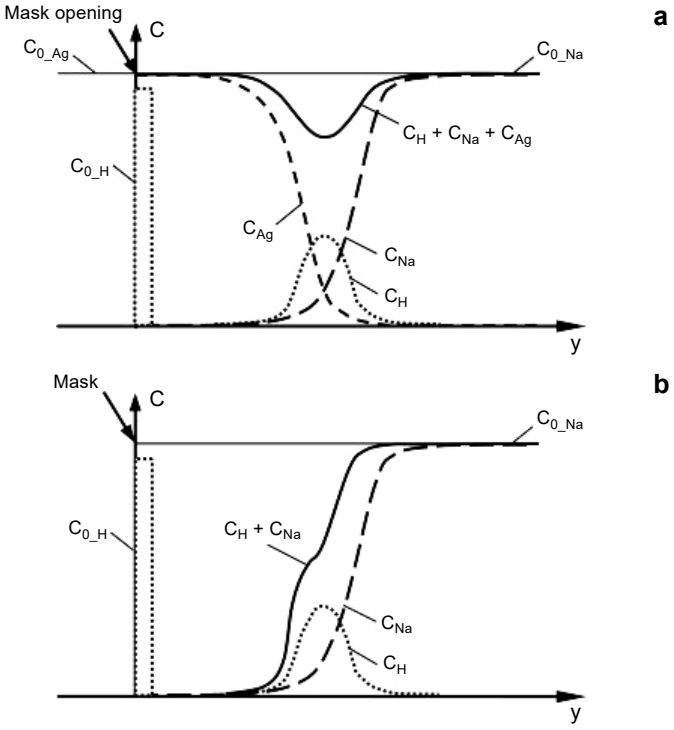


Fig. 2. Comparison of the share of $H^+$ ions in shaping the distribution of the sum of ion concentrations in glass: in mask window (**a**), and in area under the mask (**b**); $C_{0\_Na}$, $C_{0\_Ag}$ – initial concentrations of, respectively, $Na^+$ and $Ag^+$ ions, equal to $C_0$; $C_{0\_H}$ – initial concentration of hydrogen ions originating from $H_2O$ absorbed in the surface layer of glass; $C_{Na}$, $C_{Ag}$, $C_H$ – concentrations of, respectively, $Na^+$, $Ag^+$, $H^+$ ions during ion exchange.

mask, which has a thickness on the order of one micrometer. Multimode optical structures have transverse dimensions on the order of several dozen micrometers. The results of simulations indicated that such high charge density and such high field intensity as under the mask do not occur within the area of the diffusion structure in the mask's window [13]. It was therefore assumed that only mobile $Ag^+$, $Na^+$ and $H^+$ ions take part in the triple ion exchange process in this region. It was accepted that fast $H^+$ ions are found between the diffusion fronts of incoming $Ag^+$ and $Na^+$ ions flowing out into the glass (Fig. 2**a**). Since $Na^+$ ions are replaced by $Ag^+$ ions to a high degree, it was accepted that even a relatively small addition of $H^+$ ions significantly reduces space charge density in the diffusion structure formation area. Therefore, the degree of charge density reduction by $H^+$ ions should be significantly greater in the mask's window than in the layer under the mask, in which the stream of $Ag^+$ ions is not present, besides its proximity to the mask edge (Fig. 2**b**). The adoption in [12–14] of a constant value of coefficient $m$ in Eq. (4), independent of the location where the space charge is generated, was the primary cause of the inability to more accurately estimate the influence of the charge under the mask on the shape of $Ag^+$ ions' diffusion contours relative to the role of the charge in the area of the optical structure, as described in Introduction.

## 3. Proposal of modeling method

Paper [13] demonstrated that a change in the value of coefficient $m$ has a significant influence on the migration range and shape of concentration contours of $Ag^+$ ions. Coefficient $m$ was proposed as a new modeling parameter besides those used until then, including $D$, $f_H$, and $M$. A hypothesis was formulated [13] that space charge in the area of the optical structure has a greater influence on shaping the concentration contours of $Ag^+$ ions than the charge present under the mask. Verification of this hypothesis requires the adoption of different values of coefficient $m$ in the polarized layer compared to the value accepted in the optical structure, as well as the analysis of the influence of change of these values on the shape of the $Ag^+$ ion concentration contour. Therefore, determining the proper criterion for differentiation of the value of coefficient $m$ in the modeled area plays a critical role. When analyzing the characteristics of the modeled waveguides presented in [13], it can be observed that the negative charge zone of lower density is located solely within the area already encompassed by the migration range of $Ag^+$ ions. A space charge of higher density is present in the polarized layer at locations not yet reached by $Ag^+$ ions. Hence, the position of the diffusion front of silver ions can be accepted to be the natural boundary of these two areas, in which the density of the negative charge will have different values, meaning that the value of coefficient $m$ will also be different. This is particularly visible in the vicinity of the mask edge. After relatively rapid formation of a stationary polarized layer characterized by an $m$ coefficient of high value, charge density should be reduced behind the diffusion front as the range of lateral diffusion of $Ag^+$ ions increases in the direction under the mask through the adoption of a lower $m$ value.

An area through which the diffusion front of $Ag^+$ ions has passed is characterized by a silver concentration greater than zero throughout the entire ion exchange process under the set boundary condition of a constant value of silver ions in the mask's window. For the purposes of this paper, a concentration criterion for differentiation of the value of coefficient $m = f(C_{Ag})$ was proposed. At points with concentration $C_{Ag}$ less than the arbitrarily accepted value of $0.01C_0$, a high $m$ value was adopted, and at points where $C_{Ag} \geq 0.01C_0$, the $m$ value was reduced. Great significance should also be ascribed to the mathematical form of function $m = f(C_{Ag})$. Function $f(C_{Ag})$, with a stepped form, was used. A more mild, exponential graph of function $m = f(C_{Ag})$ was also proposed. Other, more complex examples of function $f(C_{Ag})$ can also be proposed. The value of coefficient $m$ should also depend on the glass substrate and the type of $Ag^+$ ions source. At this stage, the adopted proposals are only an approximation of the true dependence, which is not known in detail.

## 4. Numerical modeling

A finite difference algorithm based on the assumptions described in the previous subsections was used in numerical simulations. Finite difference explicit method was used. The derivatives in Eqs. (1), (5) were approximated by a central difference formula. A detailed description of boundary conditions and initial concentrations of $Ag^+$ and $Na^+$ ions, as well as electrical potential, presented schematically in Fig. 3, can be found in previous articles [12–14]. In particular, 100% $AgNO_3$ molten salt was presumed as a source of $Ag^+$ ions. A boundary condition of a constant value of $Ag^+$ ions concentration equal to the initial value of $Na^+$ ions concentration in glass was assumed at the surface of glass in the mask opening. A zero value of sodium ions concentration was assumed at the glass surface in this area. Boundary conditions of electric potential: a constant value $U = U_0$ at the whole top surface of glass, a zero value at the bottom side of glass and zero values of $\partial U/\partial x$ at the sides of a glass plate were assumed in numerical simulations. Only half of the ion exchange area was used for simulations due to the $y$-axis symmetry of the area. Numerical simulations were conducted using

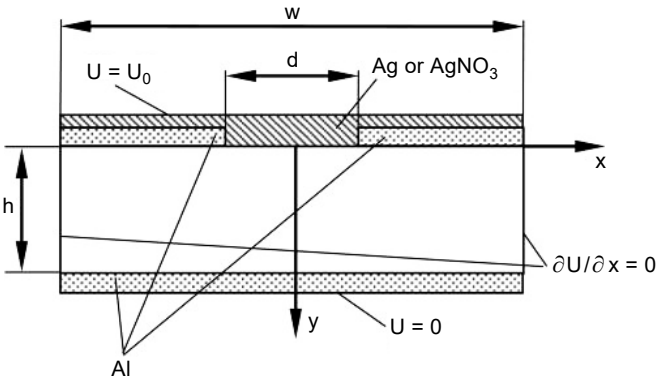


Fig. 3. Electric potential $U$ boundary conditions used in numerical simulations.

an irregular, rectangular grid with 124 and 90 nodes in the $x$ and $y$ directions, respectively. The greatest density of the grid, corresponding to a distance between nearest nodes on the order of 0.2 μm, was applied in the $y$ direction and in the near-anode area, as well as in the $x$ direction near the edge of the mask's window. The values of material parameters similar to those used for typical soda-lime glass used in experiments in [14] were adopted. The following, representative values of working parameters were used for numerical simulations:

- initial $Na^+$ ion concentration in glass $C_0 = 7300$ mol/m$^3$,
- DC voltage $U_0 = 20$ V,
- width and height of simulated area, accordingly: $w = 4.0$ mm and $h = 1.5$ mm,
- mask window width $d$ from 42 to 85 μm,
- time $t = 300$ s,
- time step $\Delta t = 5 \times 10^{-3}$ s,
- dielectric constant of glass $\varepsilon_r = 10$,
- temperature $T = 628$ K,
- self-diffusion coefficient $D_{Na}$ from $1.9 \times 10^{-14}$ to $2.5 \times 10^{-14}$ m$^2$/s,
- ratio of self-diffusion coefficients $M = D_{Ag}/D_{Na}$ from 0.3 to 0.7,
- Haven's ratio $f_H$ from 0.2 to 0.3.

T a b l e. Values of process parameters used in numerical simulations: ratio $M = D_{Ag}/D_{Na}$, Haven ratio $f_H$, self-diffusion coefficient $D_{Na}$, coefficient decreasing the density of a space charge $m(C_{Ag})$, time $t = 300$ s, and initial concentration $C_0 = 7300$ mol/m$^3$.

| No. | $M$ | $f_H$ | $D_{Na}$ ($\times 10^{-14}$ m$^2$/s) | $m(C_{Ag})$ |
|---|---|---|---|---|
| 1 | 0.7 | 0.2 | 1.9 | $m = 2.0 \times 10^{-7}$ |
| 2 | 0.7 | 0.2 | 1.9 | $m(C_{Ag} < 0.01C_0) = 2.0 \times 10^{-7}$; $m(C_{Ag} \geq 0.01C_0) = 2.0 \times 10^{-8}$ |
| 3 | 0.7 | 0.2 | 1.9 | $m(C_{Ag} < 0.01C_0) = 2.0 \times 10^{-7}$; $m(C_{Ag} \geq 0.01C_0) = 2.0 \times 10^{-9}$ |
| 4 | 0.7 | 0.2 | 1.9 | $m = 2.0 \times 10^{-7}$ |
| 5 | 0.7 | 0.2 | 1.9 | $m(C_{Ag}) = 0.90 \times 2.0 \times 10^{-7} \times \exp(-0.001\,C_{Ag}) + 2.0 \times 10^{-8}$ |
| 6 | 0.7 | 0.2 | 1.9 | $m(C_{Ag}) = 0.99 \times 2.0 \times 10^{-7} \times \exp(-0.001\,C_{Ag}) + 2.0 \times 10^{-9}$ |
| 7 | 0.7 | 0.2 | 1.9 | $m = 2.0 \times 10^{-7}$ |
| 8 | 0.7 | 0.2 | 1.9 | $m(C_{Ag} < 0.01C_0) = 2.0 \times 10^{-7}$; $m(C_{Ag} \geq 0.01C_0) = 2.0 \times 10^{-8}$ |
| 9 | 0.7 | 0.2 | 1.9 | $m(C_{Ag} < 0.01C_0) = 2.0 \times 10^{-7}$; $m(C_{Ag} \geq 0.01C_0) = 2.0 \times 10^{-9}$ |
| 10 | 0.7 | 0.2 | 1.9 | $m = 4.0 \times 10^{-7}$ |
| 11 | 0.7 | 0.2 | 1.9 | $m(C_{Ag} < 0.01C_0) = 4.0 \times 10^{-7}$; $m(C_{Ag} \geq 0.01C_0) = 2.0 \times 10^{-9}$ |
| 12 | 0.7 | 0.2 | 1.9 | $m = 1.0 \times 10^{-7}$ |
| 13 | 0.7 | 0.2 | 1.9 | $m(C_{Ag} < 0.01C_0) = 1.0 \times 10^{-7}$; $m(C_{Ag} \geq 0.01C_0) = 2.0 \times 10^{-9}$ |
| 14 | 0.7 | 0.2 | 2.5 | $m = 2.0 \times 10^{-7}$ |
| 15 | 0.7 | 0.2 | 2.5 | $m(C_{Ag} < 0.01C_0) = 2.0 \times 10^{-7}$; $m(C_{Ag} \geq 0.01C_0) = 2.0 \times 10^{-9}$ |
| 16 | 0.7 | 0.3 | 1.9 | $m = 2.0 \times 10^{-7}$ |
| 17 | 0.7 | 0.3 | 1.9 | $m(C_{Ag} < 0.01C_0) = 2.0 \times 10^{-7}$; $m(C_{Ag} \geq 0.01C_0) = 2.0 \times 10^{-9}$ |
| 18 | 0.3 | 0.2 | 1.9 | $m = 2.0 \times 10^{-7}$ |
| 19 | 0.3 | 0.2 | 1.9 | $m(C_{Ag} < 0.01C_0) = 2.0 \times 10^{-7}$; $m(C_{Ag} \geq 0.01C_0) = 2.0 \times 10^{-9}$ |

Article [13] demonstrated that a change in the value of coefficient $m$, identical throughout the entire area of the simulation, significantly affects diffusion range and the shape of $Ag^+$ ion concentration contours. In particular, a decreasing $m$ value was accompanied by the growth of the migration range of $Ag^+$ ions, both into the glass and in the lateral direction under the mask edges. In order to assess the effect of different $m$ values in the two characteristic areas described above, ion exchange was modeled for different values of parameters $D_{Na}$, $M$ and $f_H$ in this work. Function $m = f(C_{Ag})$, accepted in Section 3, was used, with the value of coefficient $m$ being changed in the region of the optical structure and left unchanged in the remaining modeled area at the same time. The selection of working coefficient values that were used is given in the Table. The majority of parameter number values are equal to those applied in [13] for the purpose of facilitating the comparison of results with those previously obtained.

## 5. Results

The Table compiles the parameter values accepted during modeling of successive variants. The results of numerical simulations are presented in Figs. 4–7. The figures also

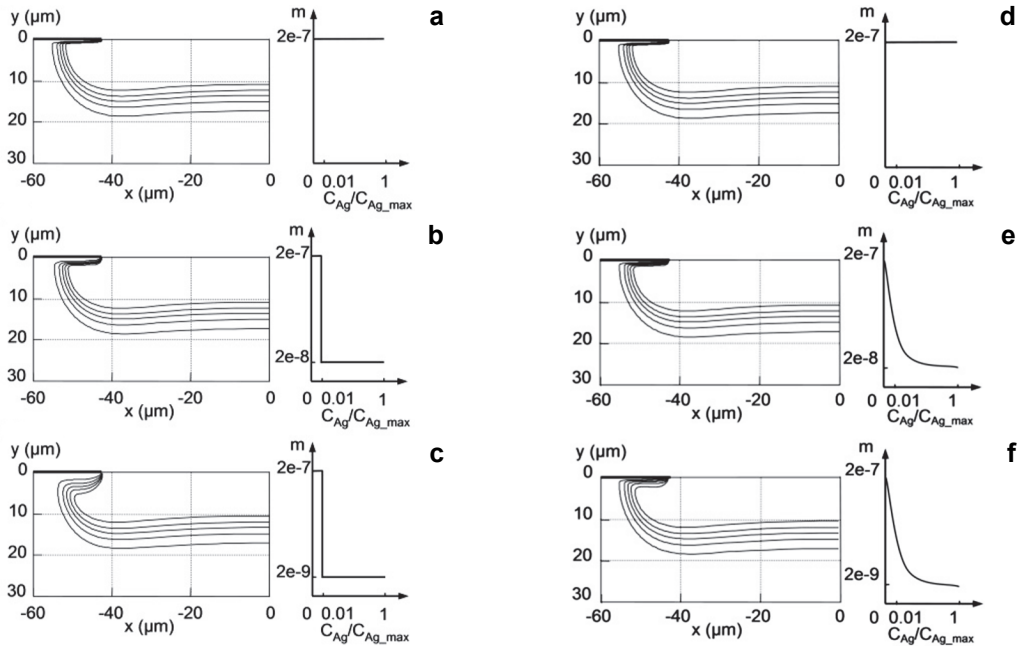


Fig. 4. The Ag concentration contour lines, in the direction to the inside of glass: $0.8C_{Ag\_max}$, $0.6C_{Ag\_max}$, $0.4C_{Ag\_max}$, $0.2C_{Ag\_max}$, $0.05C_{Ag\_max}$ ($C_{Ag\_max}$ is the maximum Ag concentration); the influence of a form of step function $m = f(C_{Ag})$ on numerical simulation results of field-assisted waveguide formation: for parameters of item No. 1 (**a**), No. 2 (**b**), and No. 3 (**c**) in the Table; the influence of a form of exponential function $m = f(C_{Ag})$ on numerical simulation results of field-assisted waveguide formation: for parameters of item No. 4 (**d**), No. 5 (**e**), and No. 6 (**f**) in the Table (only a half of each symmetrical contour is shown for clarity's sake).

contain a schematic, graphical presentation of the mathematical form of function $m = f(C_{Ag})$ used for modeling. The exponential form of function $f(C_{Ag})$ was proposed in a manner ensuring a relatively mild change of coefficient $m$ along with the change in silver concentration. As can be seen in Fig. 4, the step change of $m$ from the value of $2.0 \times 10^{-7}$ to $2.0 \times 10^{-8}$ and to $2.0 \times 10^{-9}$ upon an increase in concentration $C_{Ag}$ above $0.01C_0$ (Figs. 4**b** and 4**c**), in comparison to the applied constant value of $m = 2.0 \times 10^{-7}$ (Fig. 4**a**), results in a change of the slope of the diffusion profile of $Ag^+$ ions under the mask in the vicinity of the mask's edge. The diffusion range of $Ag^+$ ions and shapes of $Ag^+$ ion concentration contours in the glass do not change. This result suggests that the space charge within the optical structure has an influence solely on the shapes of silver concentration contours near the edges of the mask but does not affect the shape of the diffusion profile of the remaining part of the waveguide nor the range of $Ag^+$ ion diffusion into the glass. Therefore, one may draw the conclusion that the charge under the mask decides the fundamental characteristics of the waveguide's diffusion profile. The charge in the area of the diffusion structure only affects the thickness of the polarized layer under the mask's edge within the area occupied by the waveguide, visibly increasing this thickness as charge density decreases.

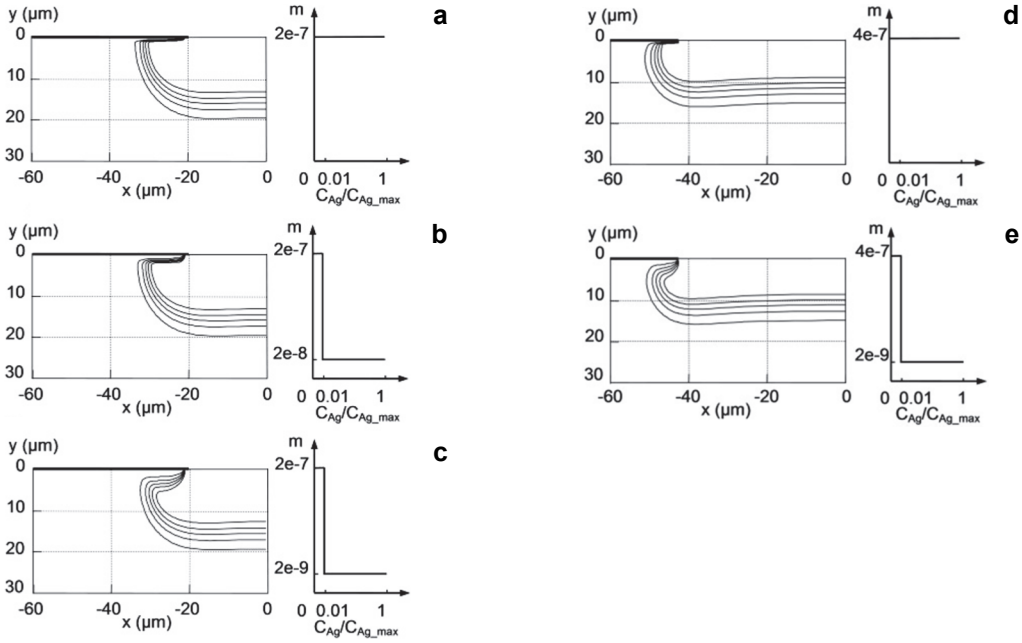


Fig. 5. The Ag concentration contour lines, in the direction to the inside of glass: $0.8C_{Ag\_max}$, $0.6C_{Ag\_max}$, $0.4C_{Ag\_max}$, $0.2C_{Ag\_max}$, $0.05C_{Ag\_max}$ ($C_{Ag\_max}$ is the maximum Ag concentration); the influence of a form of step function $m = f(C_{Ag})$ and narrower mask window on numerical simulation results of field-assisted waveguide formation: for parameters of item No. 7 (**a**), No. 8 (**b**), and No. 9 (**c**) in the Table; the influence of a form of step function $m = f(C_{Ag})$ and higher charge density under the mask on numerical simulation results of field-assisted waveguide formation: for parameters of item No. 10 (**d**), and No. 11 (**e**) in the Table (only a half of each symmetrical contour is shown for clarity's sake).

To confirm the aptness of the conclusion formulated above, a simulation was performed changing the character of function $m = f(C_{Ag})$ and changing the main parameters of the model given in the Table. Adoption of the exponential form of function $m$ =

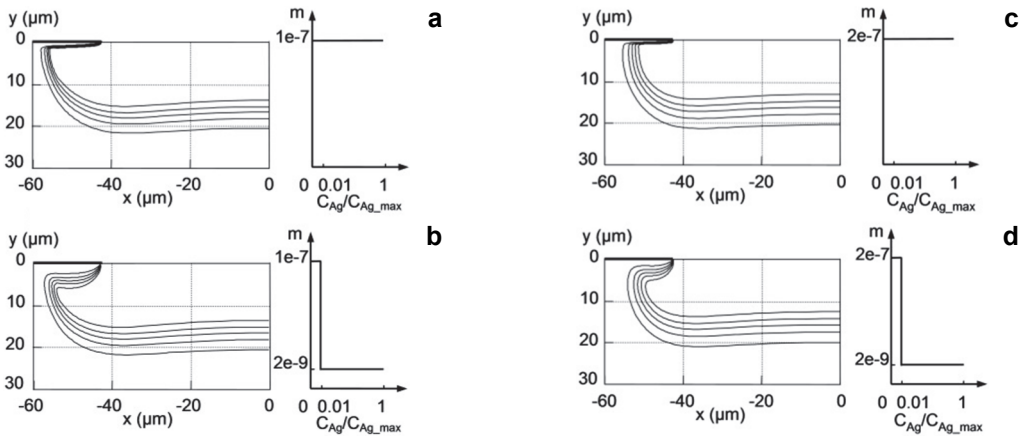


Fig. 6. The Ag concentration contour lines, in the direction to the inside of glass: $0.8C_{Ag\_max}$, $0.6C_{Ag\_max}$, $0.4C_{Ag\_max}$, $0.2C_{Ag\_max}$, $0.05C_{Ag\_max}$ ($C_{Ag\_max}$ is the maximum Ag concentration); the influence of a form of step function $m = f(C_{Ag})$ and lower charge density under the mask on numerical simulation results of field-assisted waveguide formation: for parameters of item No. 12 (**a**), and No. 13 (**b**) in the Table; the influence of a form of step function $m = f(C_{Ag})$ and self-diffusion coefficient $D_{Na}$ on numerical simulation results of field-assisted waveguide formation: for parameters of item No. 14 (**c**), and No. 15 (**d**) in the Table (only a half of each symmetrical contour is shown for clarity's sake).

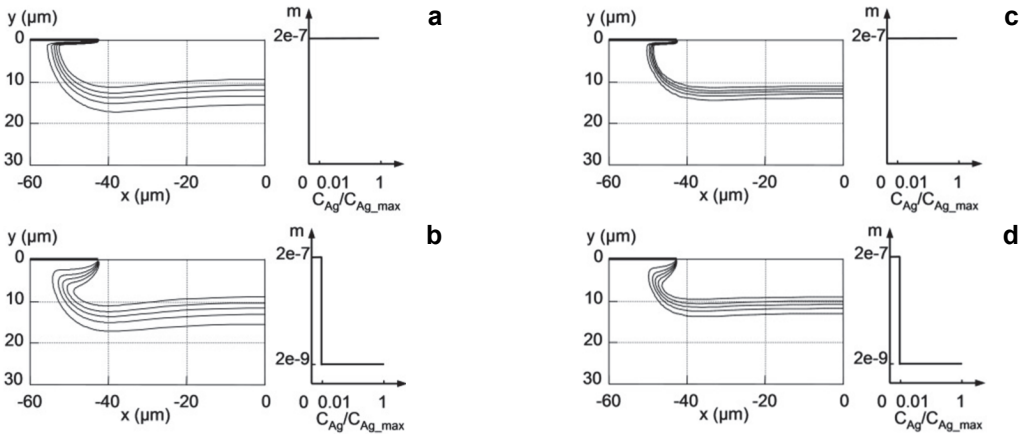


Fig. 7. The Ag concentration contour lines, in the direction to the inside of glass: $0.8C_{Ag\_max}$, $0.6C_{Ag\_max}$, $0.4C_{Ag\_max}$, $0.2C_{Ag\_max}$, $0.05C_{Ag\_max}$ ($C_{Ag\_max}$ is the maximum Ag concentration); the influence of a form of step function $m = f(C_{Ag})$ and Haven's ratio $f_H$ on numerical simulation results of field-assisted waveguide formation: for parameters of item No. 16 (**a**), and No. 17 (**b**) in the Table; the influence of a form of step function $m = f(C_{Ag})$ and coefficient $M$ on numerical simulation results of field-assisted waveguide formation: for parameters of item No. 18 (**c**), and No. 19 (**d**) in the Table (only a half of each symmetrical contour is shown for clarity's sake).

$f(C_{Ag})$ with different ranges (Figs. 4**d**–4**f**) and of stepped function $m = f(C_{Ag})$ for simulations, in the case of a narrower mask window (Figs. 5**a**–5**c**), yielded results consistent with the conclusion formulated above. In particular, simulations performed for a larger and smaller range of value change of stepped function $m = f(C_{Ag})$, with higher and lower charge density under the mask, accordingly (Figs. 5**d**, 5**e** and Figs. 6**a**, 6**b**), showed the dominant influence of the charge under the mask on $Ag^+$ ions diffusion range. The influence of the charge in the waveguide area on the shape of diffusion profile near the mask edge is also clearly visible. Results obtained for different coefficient values: self-diffusion coefficient $D_{Na}$ (Figs. 6**c**, 6**d**), Haven's ratio $f_H$ (Figs. 7**a**, 7**b**) and coefficient $M$ (Figs. 7**c**, 7**d**) also seem to confirm the conclusion formulated above. In these cases of applied $m = f(C_{Ag})$ functions, the diffusion range of $Ag^+$ ions into the glass did not change, however the slope of the diffusion profile of $Ag^+$ ions under the mask was reduced to a greater or lesser extent, suggesting an increase in the thickness of the polarized layer in this region.

## 6. Conclusions

Based on the results of the model accounting for the concentration-dependent function $m = f(C_{Ag})$, hypotheses concerning the role of space charge in shaping the waveguide's diffusion profile, formulated in previous publications [12–14], can be verified. The results of numerical simulations performed separately for different space charge densities within the area of the polarized layer under the mask and in the region of optical structure formation, made it possible to draw conclusions about the role played by the charge present in these two areas. Conducted simulations show that the charge accumulated under the mask has a fundamental influence on the shape of concentration contours and migration range of $Ag^+$ ions into the glass. The space charge in the area of the waveguide's structure, despite being situated directly in the area of $Ag^+$ ion diffusion, only affects the thickness of the polarized layer under the mask in the area of the waveguide, shaping the diffusion profile of $Ag^+$ ions at this location. Therefore, the assumption of the significant role of the charge located in the region of the diffusion structure was verified, the influence of which is limited to shaping the waveguide's diffusion profile within a relatively narrow area under the mask's edge. Nevertheless, as the mask window's width decreases, the share of the area located directly under the mask increases relative to the entire area of the optical structure. For this reason, for a sufficiently narrow mask window, the influence of charge distribution in both areas on the shape of the diffusion profile may be of similar magnitude.

The results of numerical simulations indicate a new possibility of shaping the refractive profile of channel waveguides in the production process. The change in the concentrations of admixtures affecting the space charge density in the surface layer of glass, separately in the mask opening, as well as under the mask, should influence the shape of the refractive profile of the waveguide. In particular, the reduction of the space charge density in the mask window can be easily achieved by increasing the amount of absorbed water (and therefore $H^+$ ion concentration) after the window in the mask

has been made. Varied charge density can be used as a new technological parameter of the field-assisted ion exchange process. Verification of this postulate may be an interesting research goal in a future experimental work.

*Acknowledgements* – This work was supported by Polish Ministry of Science and Higher Education (S/WM/2/2017).

## References

[1] TERVONEN A., HONKANEN S., WEST B.R., *Ion-exchanged glass waveguide technology: a review*, Optical Engineering **50**(7), 2011, article ID 071107, DOI: 10.1117/1.3559213.

[2] WEST B., *Ion-exchanged glass waveguides*, [In] *The Handbook of Photonics*, [Eds.] M.C. Gupta, J. Ballato, 2nd Ed., CRC Press, 2007, pp. 13-1–13-35.

[3] HONKANEN S., WEST B.R., YLINIEMI S., MADASAMY P., MORRELL M., AUXIER J., SCHÜLZGEN A., PEYGHAMBARIAN N., CARRIERE J., FRANTZ J., KOSTUK R., CASTRO J., GERAGHTY D., *Recent advances in ion exchanged glass waveguides and devices*, Physics and Chemistry of Glasses – European Journal of Glass Science and Technology Part B **47**(2), 2006, pp. 110–120.

[4] YUNJI YI, HUANRAN WANG, YU LIU, MINGHUI JIANG, XIBIN WANG, FEI WANG, DAMING ZHANG, *Multilayer hybrid waveguide amplifier for three-dimension photonic integrated circuit*, IEEE Photonics Technology Letters **27**(22), 2015, pp. 2411–2413, DOI: 10.1109/LPT.2015.2467175.

[5] ROTH J.-P., KÜHLER T., GRIESE E., *Low loss optical MMI-based splitter based on a semi-analytical modeling approach*, Optical and Quantum Electronics **50**(2), 2018, article ID 78, DOI: 10.1007/s11082-018-1348-9.

[6] STOSCH J.H., KÜHLER T., GRIESE E., *Analysis and optimisation of bidirectional optical couplers in PCBs*, Optical and Quantum Electronics **50**(2), 2018, article ID 109, DOI: 10.1007/s11082-018-1379-2.

[7] CASALE M., BUCCI D., BASTARD L., BROQUIN J.-E., *Hybrid erbium-doped DFB waveguide laser made by wafer bonding of two ion-exchanged glasses*, Ceramics International **41**(6), 2015, pp. 7466–7470, DOI: 10.1016/j.ceramint.2015.02.067.

[8] CHENG D., SAARINEN J., SAARIKOSKI H., TERVONEN A., *Simulation of field-assisted ion exchange for glass channel waveguide fabrication: effect of nonhomogeneous time-dependent electric conductivity*, Optics Communications **137**(4–6), 1997, pp. 233–238, DOI: 10.1016/S0030-4018(97)00013-8.

[9] ALBERT J., LIT J.W.Y., *Full modeling of field-assisted ion exchange for graded index buried channel optical waveguides*, Applied Optics **29**(18), 1990, pp. 2798–2804, DOI: 10.1364/AO.29.002798.

[10] WEST B.R., MADASAMY P., PEYGHAMBARIAN N., HONKANEN S., *Modeling of ion-exchanged glass waveguide structures*, Journal of Non-Crystalline Solids **347**(1–3), 2004, pp. 18–26, DOI: 10.1016/j.jnoncrysol.2004.09.013.

[11] TERVONEN A., *A general model for fabrication processes of channel waveguides by ion exchange*, Journal of Applied Physics **67**(6), 1990, pp. 2746–2752, DOI: 10.1063/1.345440.

[12] MROZEK P., *Numerical and experimental investigation on $Ag^{+}$–$Na^{+}$ field assisted ion-exchanged channel waveguides*, Applied Optics **51**(20), 2012, pp. 4574–4581, DOI: 10.1364/AO.51.004574.

[13] MROZEK P., *Numerical modeling of field-assisted ion-exchanged channel waveguides by the explicit consideration of space-charge buildup*, Applied Optics **50**(22), 2011, pp. 4499–4508, DOI: 10.1364/AO.50.004499.

[14] MROZEK P., MROZEK E., LUKASZEWICZ T., *Side diffusion modeling by the explicit consideration of a space-charge buildup under the mask during strip waveguide formation in the $Ag^{+}$–$Na^{+}$ field-assisted ion-exchange process*, Applied Optics **45**(4), 2006, pp. 619–625, DOI: 10.1364/AO.45.000619.

[15] KNOWLES K.M., VAN HELVOORT A.T.J., *Anodic bonding*, International Materials Reviews **51**(5), 2006, pp. 273–311, DOI: 10.1179/174328006X102501.

[16] Krieger U.K., Lanford W.A., *Field assisted transport of $Na^+$ ions, $Ca^{2+}$ ions and electrons in commercial soda-lime glass I: experimental*, Journal of Non-Crystalline Solids **102**(1–3), 1988, pp. 50–61, DOI: 10.1016/0022-3093(88)90112-3.

[17] Lepienski C.M., Giacometti J.A., Leal Ferreira G.F., Freire Jr. F.L., Achete C.A., *Electric field distribution and near-surface modifications in soda-lime glass submitted to a DC potential*, Journal of Non-Crystalline Solids **159**(3), 1993, pp. 204–212, DOI: 10.1016/0022-3093(93)90224-L.

*Received August 30, 2018*
*in revised form October 16, 2018*